

Structural appraisal of baja prototype using resistive strain gauges and linear potentiometer

Avaliação estrutural de protótipo baja através extensômetros resistivos e potenciômetro linear

Article Info:

Article history: Received 2023-11-02 / Accepted 2024-01-20 / Available online 2024-01-24

doi: 10.18540/jcecv110iss2pp18172



Pablo Miguel Maia Pires

ORCID: <https://orcid.org/0000-0003-0592-3587>

Universidade Federal de São João del-Rei, Brazil

E-mail: pabllomiguel_26@aluno.ufsj.edu.br

José Antônio da Silva

ORCID: <https://orcid.org/0000-0003-4813-1029>

Universidade Federal de São João del-Rei, Brazil

E-mail: jant@ufsj.edu.br

Júlio César Costa Campos

ORCID: <https://orcid.org/0000-0002-9488-8164>

Universidade Federal de Viçosa, Brazil

E-mail: julio.campos@ufv.br

Antônio Marcos de Oliveira Siqueira

ORCID: <https://orcid.org/0000-0001-9334-0394>

Universidade Federal de Viçosa, Brazil

E-mail: antonio.siqueira@ufv.br

Resumo

Toda máquina ou componente estrutural sofrem uma determinada deformação elástica quando expostos a algum tipo de carga ou força, e quando se trata de projeto e validação de componentes, uma análise estrutural tem um papel fundamental, haja vista a necessidade de garantir a integridade das peças projetadas. Para isso, é eminente a imprescindibilidade de dados confiáveis para que todo o processo seja realizado de maneira coerente, pautada em critérios de engenharia. Dentro desta perspectiva, o presente estudo busca a aquisição de cargas e forças, dinâmicas ou estáticas, que estão presente em componentes principais e críticos em um protótipo tipo BAJA, da Equipe KomiKeto Baja - UFSJ, visando a aquisição de dados para utilização de condições de contorno em simulações numéricas, além de captações dinâmicas de ciclos de carregamento para posterior análise de fadiga.

Palavras-Chave: Aquisição de Dados, Protótipo Tipo Baja, Condição de Contorno, Análise Estrutural.

Abstract

Every machine or structural component undergoes a certain elastic deformation when exposed to some type of load or force. Furthermore, when it comes to the design and validation of components, a structural analysis plays a fundamental role, given the need to guarantee the integrity of the designed parts. To achieve this, reliable data is essential so that the entire process can be carried out in a coherent manner, based on engineering criteria. Therefore, the present study seeks to acquire dynamic or static loads and forces, which are present in main and critical components in a BAJA-type prototype, from the KomiKeto Baja Team - UFSJ, aiming to acquire data for the use of boundary conditions in numerical simulations, in addition to dynamic capture of loading cycles for subsequent fatigue analysis.

Keywords: Data Acquisition, Baja Prototype, Boundary Condition, Structural Analysis.

1. Introduction

Obtaining load data on mechanical components in the automotive area is being every day more explored and valued in order to carry out projects with boundary conditions that are increasingly faithful to the physical-mechanical behavior of these components, when exposed in full operation, and, thus, making it possible to optimize and increase the structural reliability of the project as a whole (Carneiro, 2019). In this sense, aiming to understand the active efforts and the dynamic behavior of the components of the KB09 prototype of the KomiKeto Baja UFSJ Team, this work presents techniques used to acquire data (loads) through strain gauge sensors and effort and load data obtained in tests and trials carried out, which are used for numerical simulations using the finite element method to validate and design vehicle components. Furthermore, the main aim is to show the results obtained, the challenges encountered and to cooperate so that new work can be carried out by other competition teams in the same field, given the scarcity of available materials focused on the topic.

1.1 Elasto-linear correlation between metallic materials and extensometers

Based on the fundamental concept of deformation (Norton, 2011), when a body is exposed to external loads, it experiences tensions corresponding to such efforts, thus generating changes in its shape in multiple directions (Figure 1).



Figure 1- Illustration of a body undergoing deformation. Source: Authors (2024).

In this way, linear deformation can be defined as the ratio between the variation in the length of a given body under analysis by its original (non-deformed) length. Thus, the following relationship can be obtained:

$$\varepsilon = \frac{\Delta L}{L} \quad (1)$$

Based on these concepts, it is possible, in parallel, to obtain a relationship between the elastic deformation experienced by the material with the variation in electrical resistance when strain gages are subjected to a given input voltage, which, when arranged in a *Wheatstone bridge*, allows determine the instantaneous resistance of the given extensometer. It is worth mentioning that, in the *Wheatstone bridge*, the complement of the bridge is normally done by resistors that suit the experiment carried out when using data acquisition modules.

From a given load applied to the component, be it compression or tension and, consequently, on the extensometer, its resistance will be modified, increasing or decreasing it, proportionally to the elastic deformation of the material, following the following equation:

$$\frac{\Delta R}{R} = K_s * \varepsilon \quad (2)$$

such that it K_s represents the sensitivity factor of the extensometer, R the original resistance, ΔR the variation of this resistance and ε the elastic deformation of the material.

1.2 Wheatstone bridge

The functioning of the *Wheatstone Bridge*, Figure 2, is done by comparing an input voltage (bridge excitation) with the output voltage. If R_1 , R_2 and R_3 are known (pre-installed in the data acquisition module hardware), it is possible to determine the value of R_1 , such that:

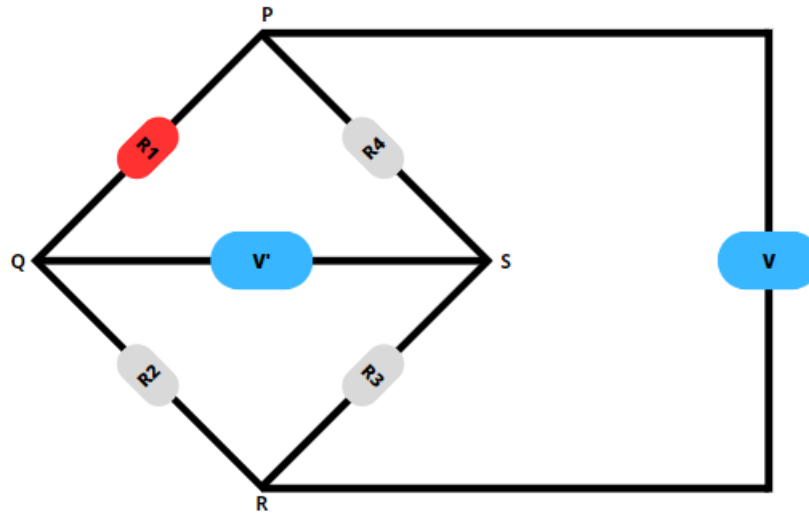


Figure 2- Illustrative representation of a Wheatstone bridge circuit. Source: Authors (2024).

$$V' = \left[\frac{R_1}{(R_1+R_2)} - \frac{R_4}{(R_4+R_3)} \right] V \tag{3}$$

where R_1 represents the resistance of the extensometer; R_2 , R_3 and R_4 are the known resistors; V is the input voltage and V' the output voltage. If R_1 there is a variation ΔR arising from the material-gage strain, we have:

$$V' = \left[\frac{(R_1 + \Delta R)}{(R_1 + \Delta R) + R_2} - \frac{R_4}{(R_4 + R_3)} \right] V \tag{4}$$

Knowing that R_2 , R_3 and R_4 have the same resistance values, therefore;

$$V' = \left[\frac{(R + \Delta R)}{(R + \Delta R) + R} - \frac{R}{2R} \right] V \tag{5}$$

since R will be significantly greater than ΔR , then;

$$V' = \frac{1}{4} \frac{\Delta R}{R} V \tag{6}$$

and so, relating to equation (2), we finally have that:

$$V' = \frac{K_S \epsilon V}{4} \tag{7}$$

Therefore, it can be concluded that the output voltage is directly proportional to the sensitivity factor (K_S) of the extensometer, the elastic deformation experienced (ϵ) and the input voltage (V); and thus, it is possible to determine such output voltage (V') and relate the material-gage behavior to acquire the tensions or loads acting on the components through linear regression and formulations

(Lee *et al.*, 2011). This bridge system, which applies to each extensometer used, is done automatically by the module (LYNX ADS 2500).

2. Methods

2.1. Installation

The preparation process for component extensometer instrumentation is important and must be followed strictly in order to obtain an accurate result (Hoffmann, [sd]). Therefore, according to manuals and *data-books* made available by the companies HBK, *Micro-Measurements – VPG* and *National Instruments*, plus a report (“Ankara Yıldırım Beyazıt Üniversitesi”, [sd]), the entire gage process of installation on components was standardized through a sequence prepared by the team members, following the NBR ISO 7500-1 and the tutorial by *Micro-Measurements – VPG: Strain gage installation on a shaft for torque measurement* (2018), in the following order:

1. Component disassembly
2. Surface cleaning of excess residue
3. Sanding (180 – 240 – 320 respectively)
4. Cleaning with isopropyl alcohol and gases
5. Final cleaning with flexible swabs
6. Marking the gluing location of the extensometers
7. Positioning the sensors on the bench with transparent tape
8. Positioning the tape with extensometer on the piece to which it will be glued and final alignment
9. Adhesive application
10. Press with your thumb for 2 minutes to bond.
11. 30 min curing time
12. Removing the transparent tape
13. Application of transparent silicone to protect each sensor
14. Installation and soldering of wires to sensor terminals

Based on the Brazilian standard NBR ISO 7500-1 and the European standard BS EN ISO 9513:2012, the entire calibration process was carried out in order to obtain a linear regression of the relationship between the strain gauge deformation, the voltage variation read by the data acquisition module and the correlated value of the known weights used.

2.2. Instrumental Arrangement

To acquire all the data in the present work, whether quasi-static (*drop-test*) or dynamic (driving on a test track), based on (Pereira, 2019), an instrumental arrangement was used, Figure 3, with the following equipment:

- 12V 60Ah car battery
- APC Back-UPS 600 UPS
- LYNX ADS2500 Acquisition Module
- Linear displacement potentiometer
- Extensometers connected in $\frac{1}{4}$ bridge (strain gages)
- Sleeve Cable AWG 4x26
- Flexible Electrical Cable 2.5mm

Thus, the power supply system was located on the floor of the prototype, as shown in Figure 4 (c), and the laptop with the LYNX ADS2500 Module in a backpack, which in turn was placed on the pilot's chest.

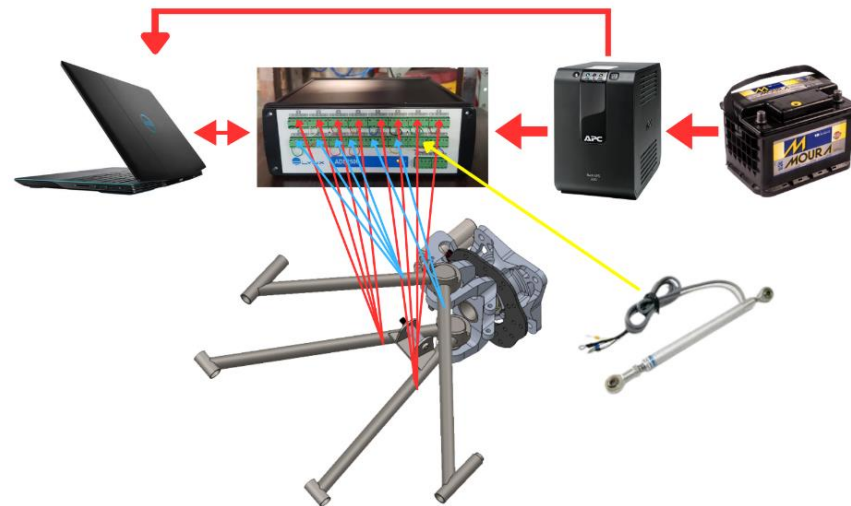


Figure 3 – Instrumental arrangement used for dynamic capture. Source: Authors (2024).

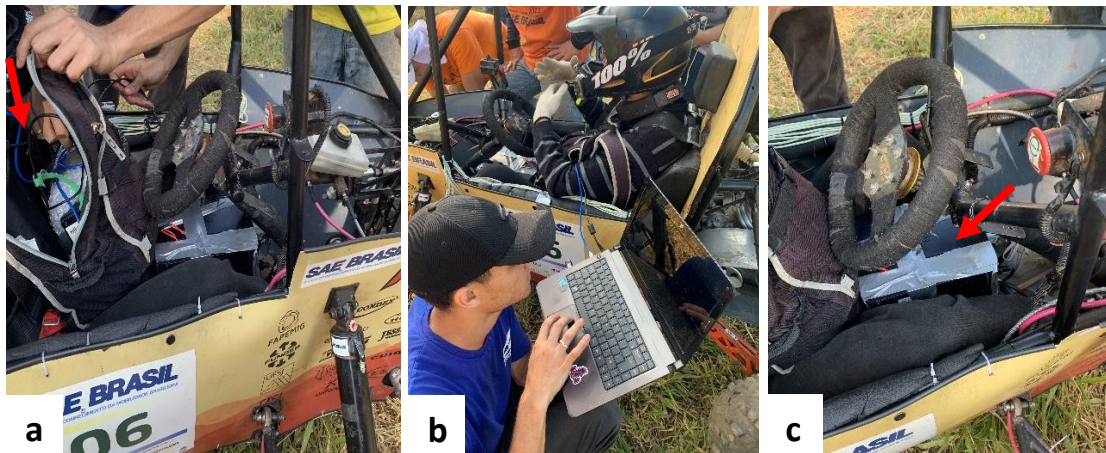


Figure 4 – Arrangement of the module and laptop in a backpack (a), configuring data recording in the LYNX SignalVista software (b) arrangement of the battery and UPS on the floor of the prototype (c). Source: Authors (2024).

2.3. Application on front suspension

For the trays, they were clamped in a vise with the aid of steel frame, based on a generic numerical simulation using finite elements, with any arbitrary force, to identify the region with the greatest gradient of deformation concentrator and, thus, A series of known weights (washers) were inserted (4,815kg, 5,380kg, 10,235kg respectively, Figure 8) in order to plot a linear regression. Figure 6, which would parameterize the equation from which the efforts (N) would be described later in dynamic tests, since the static characterization of the calibration is carried out to interpret the application of strain gauges and their due physical outputs of variation of electrical properties (electrical voltage) due to variation in mechanical properties (linear deformation). Furthermore, to guarantee the entire gluing process of the extensometers and obtain more reliable final results (Hoffmann, [sd]), a hysteresis analysis was carried out on each of the extensometers, as shown in Figure 7.

Finally, the damping course was instrumented with the aid of a linear potentiometer (Image 5-e), where it was fixed through label extensions, ensuring precise operation and obtaining the real displacement of the pneumatic damper used in the team. in order to understand the efforts absorbed by the component (Gillespie, 2021), (Silva, 2020), and use them as a comparison parameter with

the dynamic loading data obtained by the gages.

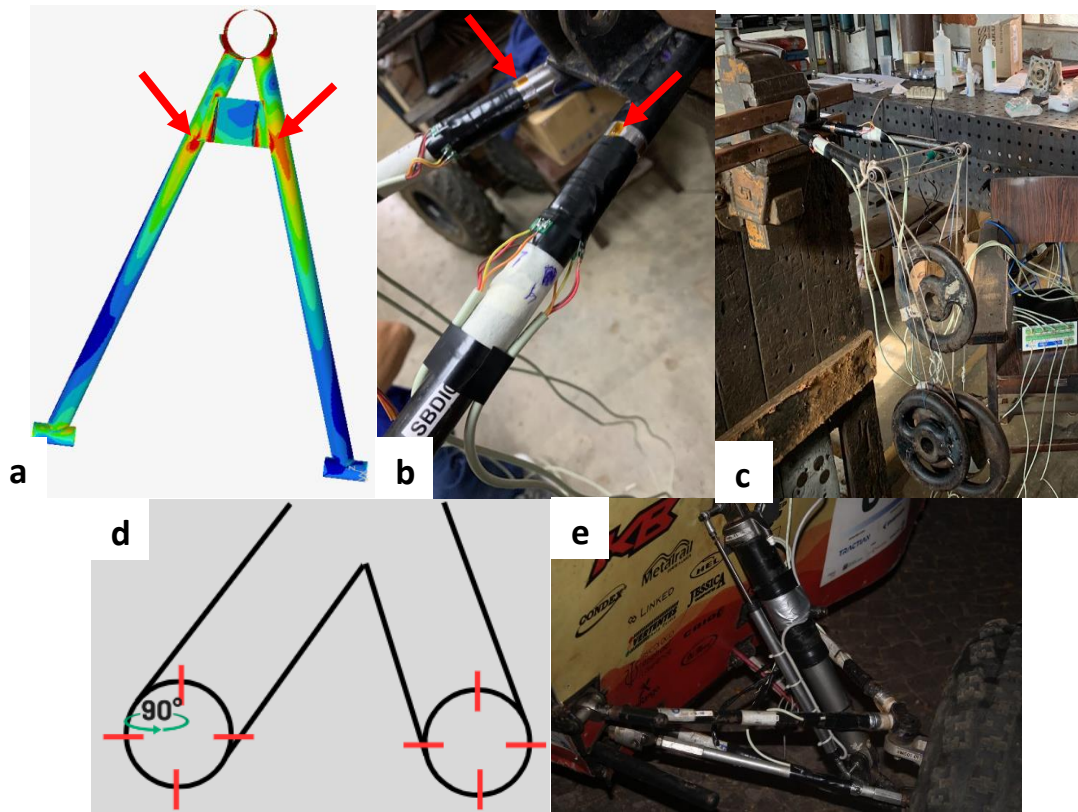


Figure 5 - Finite Element Simulation in HyperWorks software (a); gluing position of the strain gauges (b); illustration of the tray with the calibration weights (c); representation of the cross section of the tray tubes and the gluing position of the extensometers in a 1/4 bridge model (d); instrumentation of the dampers using a linear potentiometer; Linear potentiometer installed on the front shock absorber (e). Source: Authors (2024).

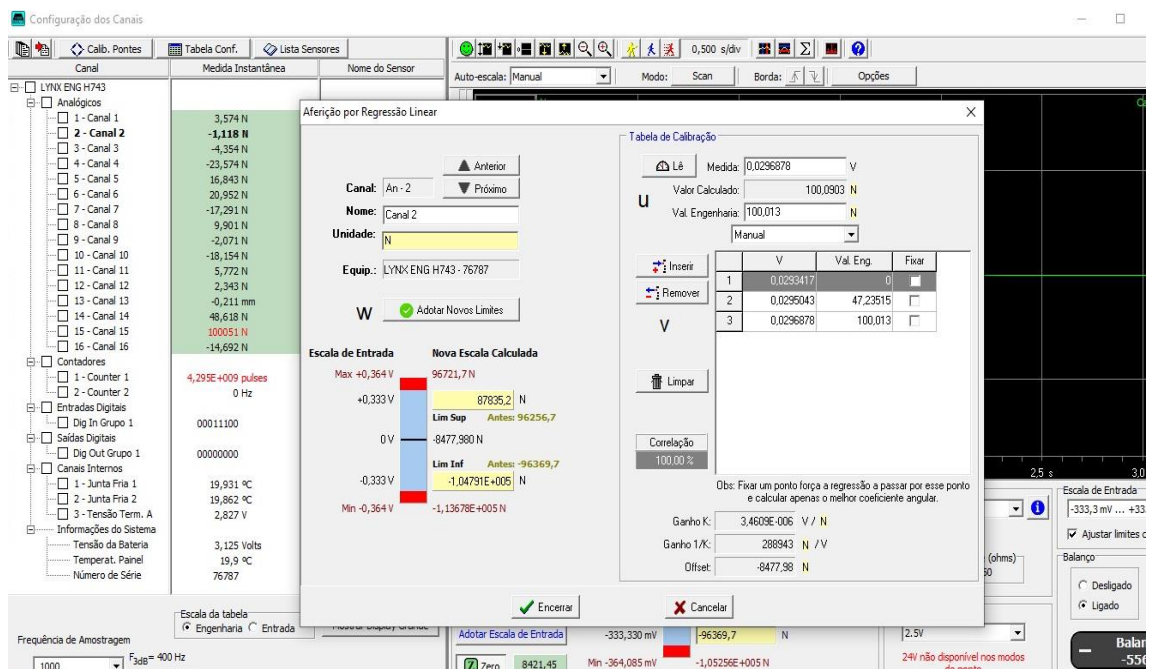


Figure 6 – Linear Regression illustration of the sensor calibration process. Source: Authors (2024).

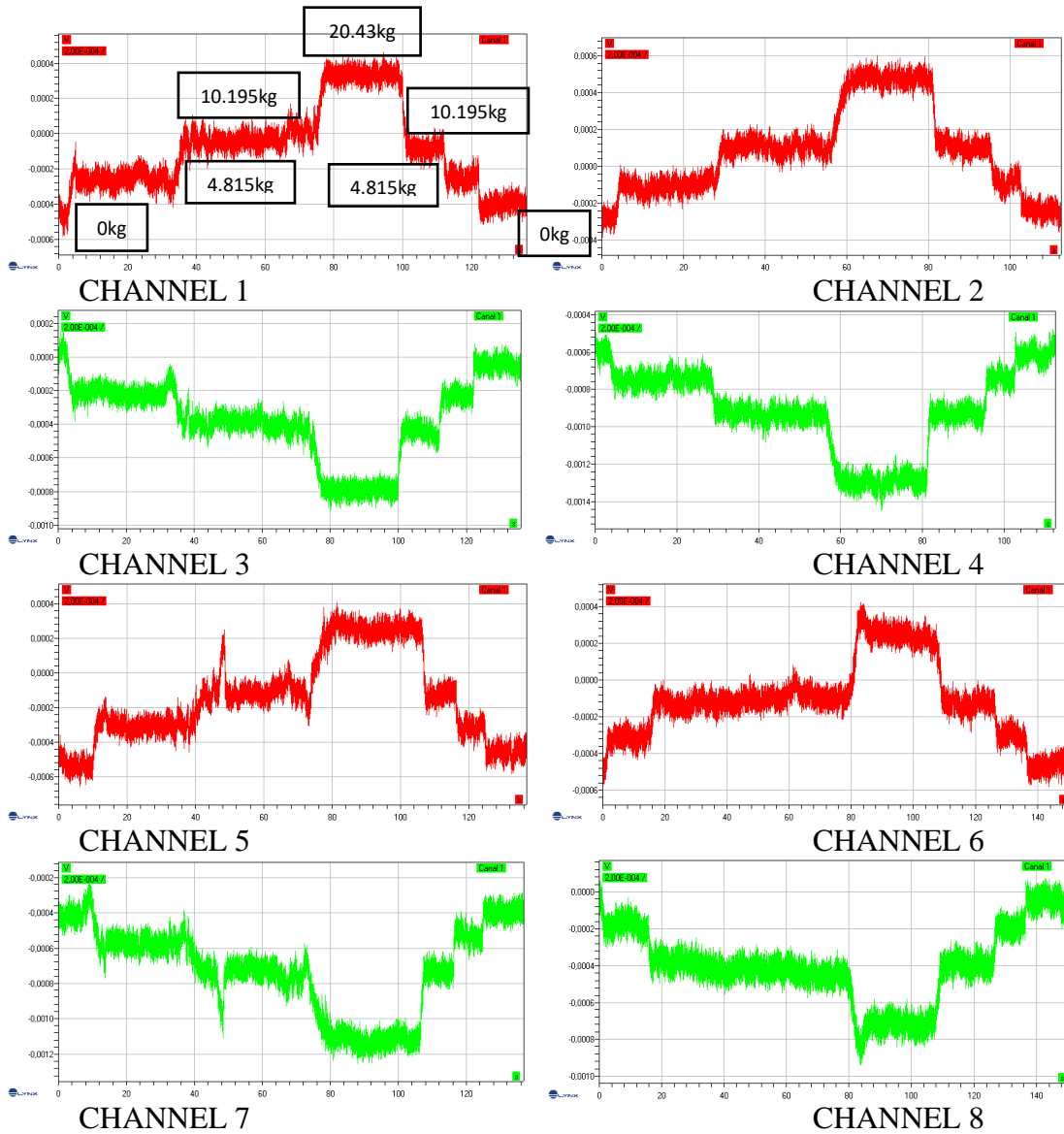


Figure 7 - Hysteresis performed on strain gauges to measure function. Source: LYNX Signal Review.



Figure 8 - Standard weights used in calibration (4,815kg, 5,380kg, 10,235kg respectively). Source: Authors (2024).

Based on the concepts of Beckwith *et al.* (1993), calculations can be carried out in order to extract the effort to which the section (tubular in the case of the present work) is being subjected. The configuration of gauges glued in a $\frac{1}{4}$ bridge when added to the signals from sensors glued on opposite faces delivers the result of the axial force present in the body under analysis; When the signals are subtracted, we have the result of shear forces, Figure 9.

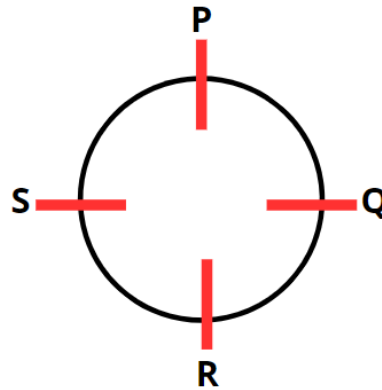


Figure 9 – Strain gluing position gauges in the cross section (tube). Source: Authors (2024).

Thus, in Figure 9, the letters P, Q, R and S are uniaxial *gages* glued to a $\frac{1}{4}$ bridge, so: $N_{axial} = (P + R)/2 = (Q + S)/2$, since when subjected to flexion, the section will nullify the shear loads since the signal obtained by the gauges will have opposite value depending on the bending criteria of the materials, and the axial loads are added together, so they must be divided by two in order to obtain the correct value. The vertical shear loads will be given by: $V_{vertical} = (P - R)/2$, since the normal loads will now cancel each other out and the shear loads of opposite signs will add up; Similarly, the horizontal shear loads will be given by: $V_{horizontal} = (S - Q)/2$.

2.4. Test Track

In order to obtain signs of durability that represent the critical working condition of the prototype, as mentioned by Carneiro in 2019, a durability route was carried out on the official test track of the Komiketo Baja Team – UFSJ, Figure 10, where it represents reliably the conditions of national and regional competition tracks, to which the car is exposed.

Unlike production line cars, Baja prototypes are not allowed to travel on highways or urban circuits, therefore, street routes, misused routes and drivability routes must be adapted for the present study (Carneiro, 2019). Therefore, a single route for continuous use is considered, representing the competition endurance route, Figure 6, where the conditions under which the prototype is exposed in an exclusive and critical way will be analyzed, that is, a route on dirt terrain with steep obstacles, ramps and ditches.

Obtaining such dynamic loads through durability signals or blocks is fundamental for the design of reliable and optimized components (Spinelli, 2012).

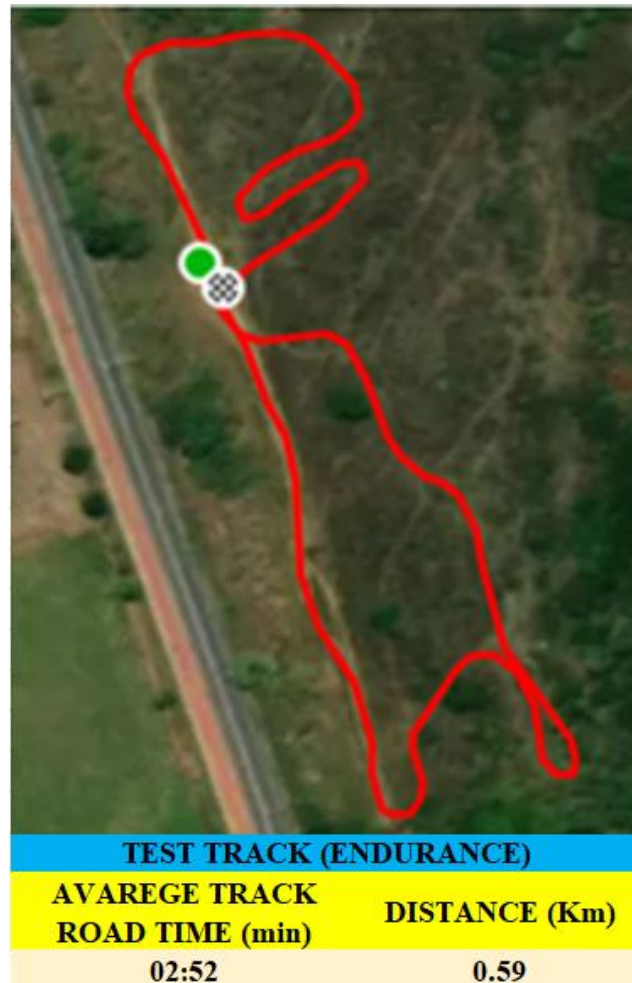
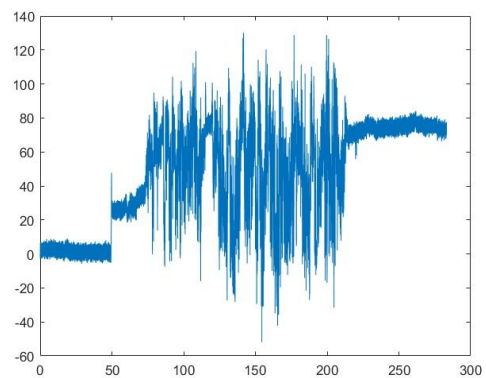
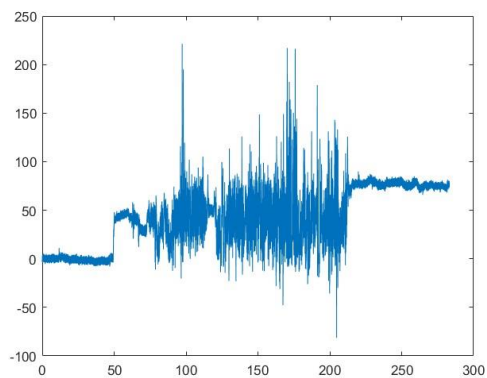
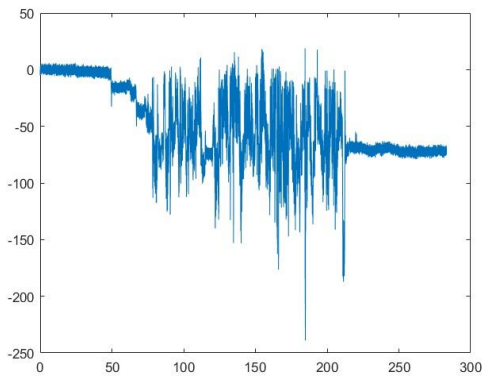
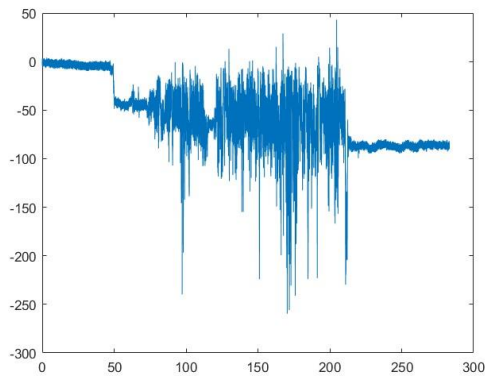
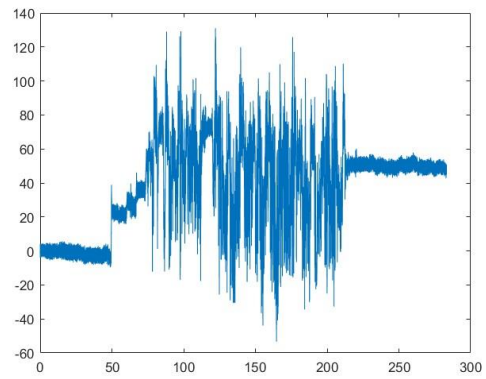
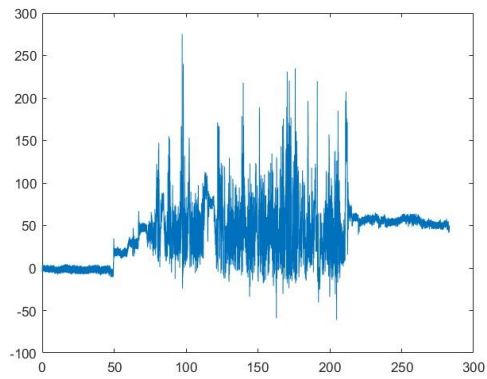
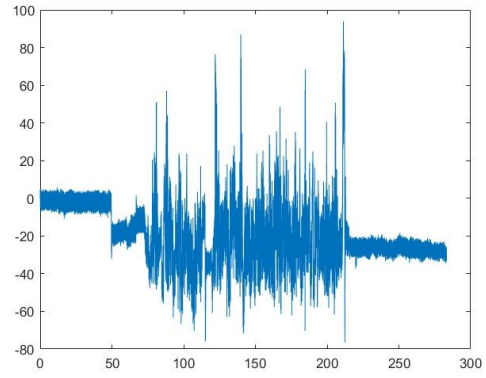
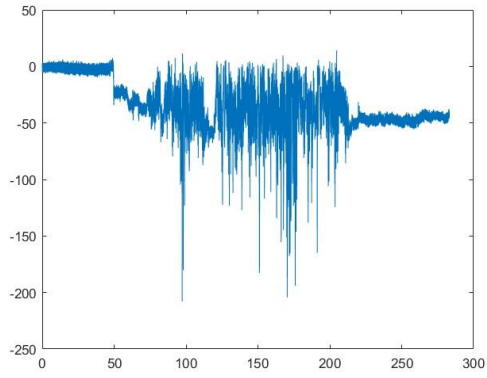


Figure 10 - Continuous use route (endurance) mapped on GPS. Source: Authors (2024).

3. Results

3.1. Test Track

Obtaining such dynamic loads through durability signals or blocks is fundamental for the design of reliable and optimized components (Spinelli, 2012). After acquiring the dynamic data taken on the test track and obtaining a block of loads (N) specific to the trace made, Figure 10, the signals were processed with the aid of the *MATLAB software*, where the signals were filtered and removed. the graphics (N - s) of each channel (represented by the letters C1, C2, Cn) of the module individually. Figure 11. In order to guarantee the reliability of the bonding and sensor behavior, all deformation relationships in opposite directions consequently generate efforts in opposite directions, which can be seen in the images below together, that is, channels 1-3; 2-4; 5-7; 6-8; 9-11; 10-12; 14-16; they have the same deformation ratio, but in opposite directions, and so on, given the gluing of the gages ($\frac{1}{4}$ of the *Wheatstone bridge*). Furthermore, a table was created in the Excel software in order to combine the sensors into axes, the sum of the efforts captured by the gauges and the relationship between them, as illustrated in Figure 12.



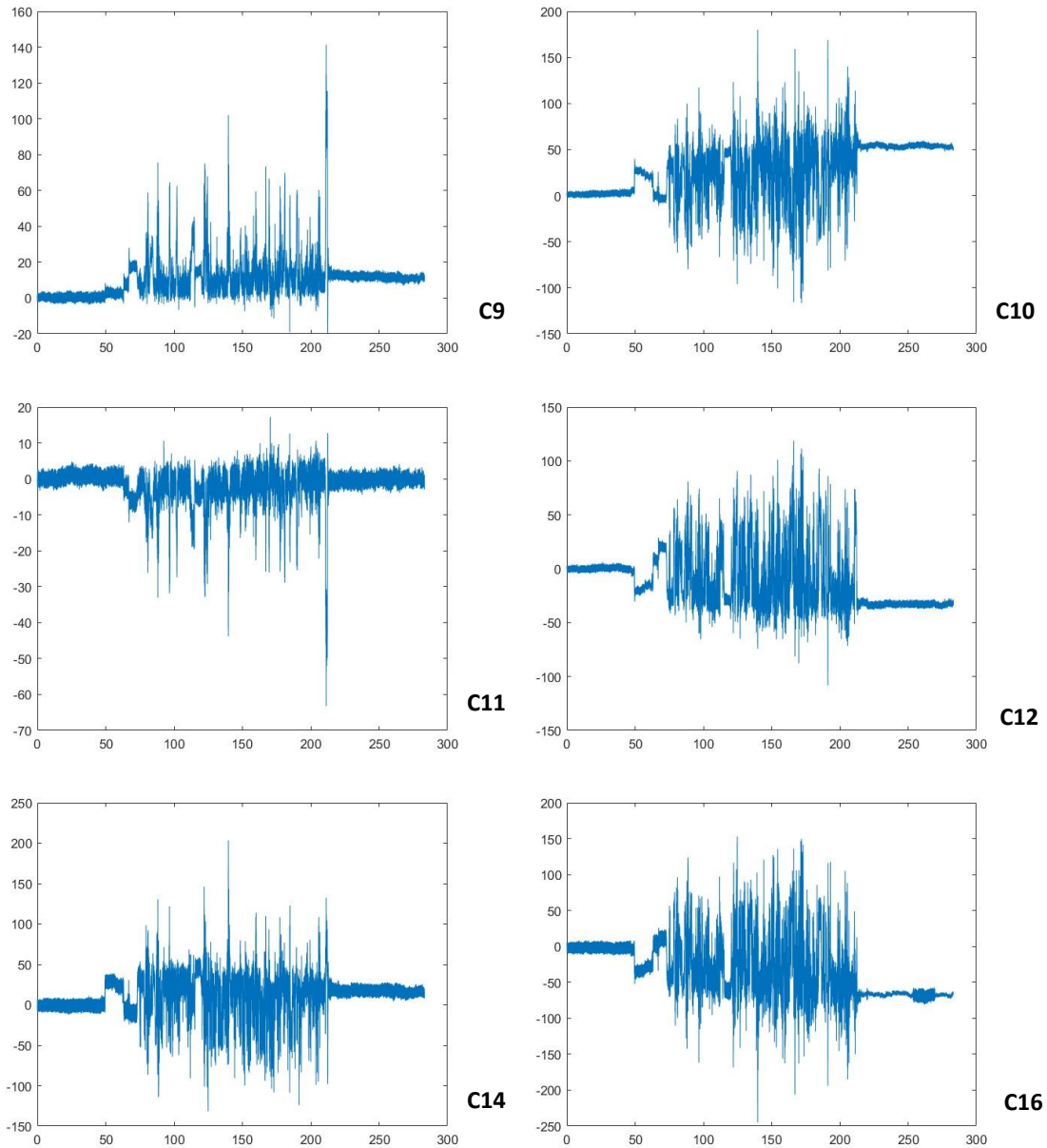


Figure 11 – Dynamic load signals captured by each extensometer glued to the suspension trays on the enduro track. Source: Authors (2024).

Then applying the system of combining the efforts captured individually by the gages in an Excel table and making the appropriate relationships N_{axial} ; $V_{vertical}$; $V_{horizontal}$, the maximum values found in the single block of dynamic signals are explained in Figure 12.

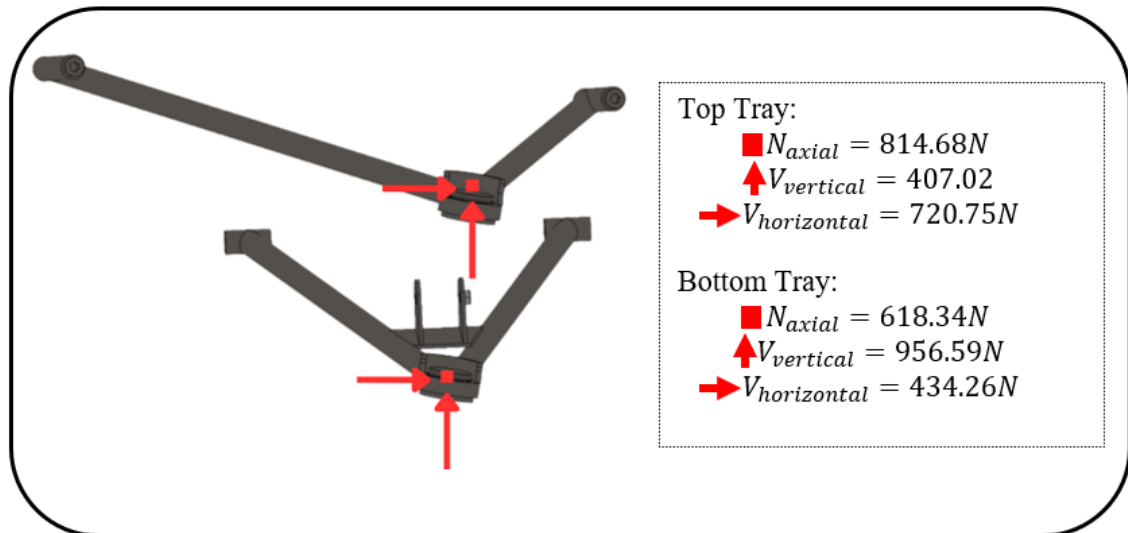


Figure 12 – Maximum dynamic load signals captured on each axis. Source: Authors (2024).

Furthermore, with the loading obtained through the linear potentiometer, Figure 5e, installed in the prototype dampers, it was possible to estimate the damper reaction load over time using the elastic force equation, Hooke's Law (Lee *et al.*, 2011). Obtaining the damping coefficient (K) of the shock absorber used in the prototype was taken from laboratory testing and will be omitted from the present work for confidentiality reasons.

$$F = K * x, \quad (8)$$

where:

F: shock absorber energy absorption force (N)

K: spring elastic constant (N/m)

x: shock absorber stroke displacement (m)

In this way, we have the loading results (N) for the time (s) of the load absorbed by the shock absorber, during the prototype's passage on the test track, illustrated in Figure 13. The maximum force obtained by this relationship was 1055.86N.

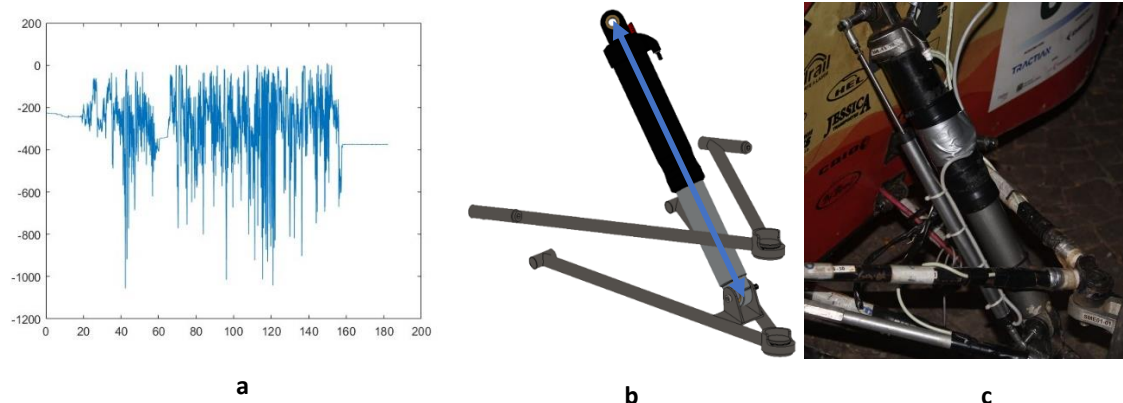


Figure 13 – Load signals (N) over time (s) obtained by the linear potentiometer (a); CAD illustration of the trays and the location of the potentiometer indicated by an arrow (b); Physical assembly for system testing (c). Source: Authors (2024).

3.2. Drop-test Data

In order to compare the accuracy of the dynamic physical data captured on the test track, below is a comparison between a *drop - test carried out at a height of 1.5m in the Adams View software* with the real *drop - test carried out at the University*, Figure 14.

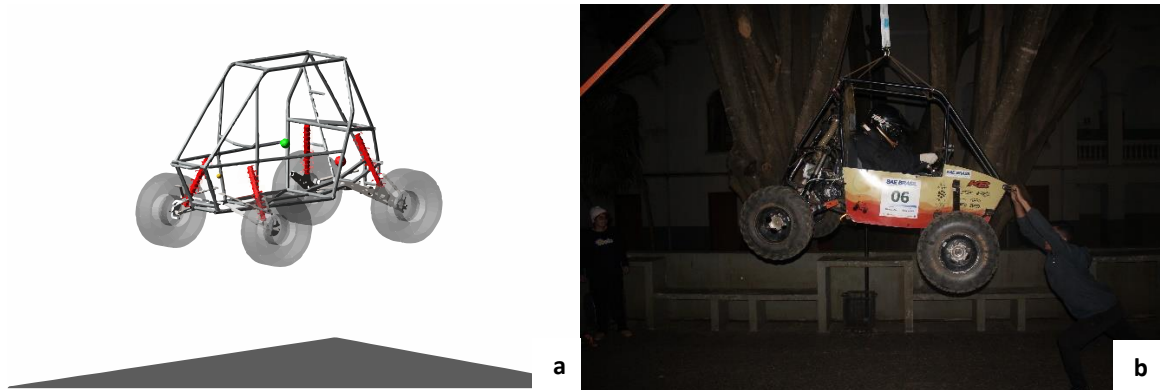


Figure 14 – Prototype at 1.5m in Adams View software for virtual drop-test (a); Prototype being lifted 1.5m for the real/physical drop-test at the University. Source: Authors (2024).

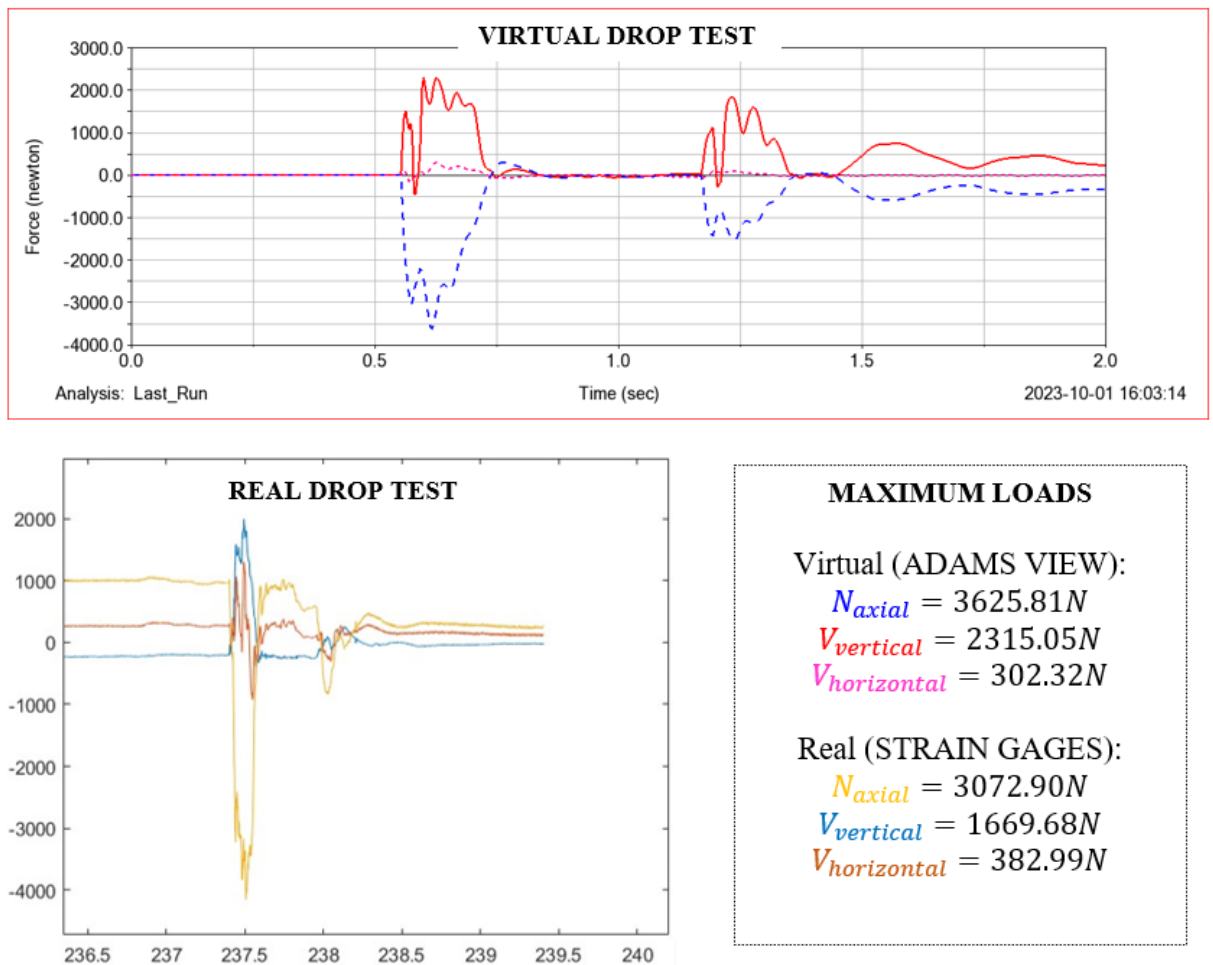


Figure 15 – Illustration and comparison between results obtained in the virtual drop-test and real/physical drop-test. Source: Authors (2024).

Explained in Figure 15 by real/physical *drop-test* carried out with the gauges, when the prototype was hanging, there is an initial tension, mainly in the axial force, which occurred due to the lack of consideration of the self-weight of the prototype and driver before resetting the sensors with the car in static deflection, i.e., standing on a flat floor; the same happens with the other components in a less significant way. Furthermore, the horizontal axis has high values of time (s) due to the time spent storing the laptop and the module inside a backpack hanging on the pilot's chest; lift the car 1.5m and hold it until it is balanced in the air; however, the data of interest is obtained in less than 1 second, which is the time for the prototype to fall.

In this way, comparing the results obtained between the virtual *drop-test using the ADAMS VIEW software and the drop physical test* carried out by members of the structural calculation sector of the team, an accuracy estimates of approximately 82% is estimated, an acceptable value according to work already carried out in this area, such as that of Pereira (2019) and Cunningham (2019).

4. Conclusion

The strain gages used are high sensitivity and precision sensors, making it possible to obtain quality results, resulting in a certainty of 82% of the results when comparing simulated data and experimental data. The results of the efforts recorded were satisfactory, which is corroborated by previous experiments carried out by Pereira (2019), and Cunningham (2019), remaining within the same order of magnitude as these other works. This demonstrates that the methodology adopted is robust and reliable. Due to the geometric complexity of the components, the application of strain gauges to tubular sections did not allow data to be obtained at the rear of the prototype.

The next work to be carried out will consist of carrying out additional validation using MEMS accelerometers and the same data acquisition module, both from LYNX company, with the purpose of quantifying the efforts on the front and rear axles. This analysis aims to compare the results obtained through accelerometry with data previously obtained through extensometry.

Finally, will also seek to develop a methodology for analyzing fatigue in the prototype's suspension components, which are subject to critical and cyclical loads arising from the contact between the tire and the ground. This analysis will be carried out based on data obtained through extensometry and/or accelerometry.

Acknowledgments

To LYNX TECNOLOGIA for the massive support with their products and software.

To Structural Calculation Sector from Komiketo Baja Team for the opportunity to get this work.

This paper was carried out with the support of the Higher Education Personnel Improvement Coordination - Brazil (CAPES) – Financing Code 001, Minas Gerais State Research Support Foundation (FAPEMIG) and Arthur Bernardes Foundation (FUNARBE).

References

- Ankara Yıldırım Beyazıt Üniversitesi. (n.d.). Strain Measure by Using Strain Gages. [Www.aybu.edu.tr](http://www.aybu.edu.tr).
https://www.aybu.edu.tr/bolumroot/contents/muhendislik_makina/files/STRAIN%20MEASUREMENT%20BY%20USING%20STRAIN%20GAUGE.pdf
- Beckwith, T. G., Marangoni, R. D., & Lienhard, J. H. (1993). *Mechanical Measurements*. Prentice Hall.
- Carneiro, G. C. (2019). *Desenvolvimento de metodologia para otimização dinâmica e estrutural de suspensão veicular traseira do tipo eixo de torção*. Tese de Doutorado, Universidade Federal de Minas Gerais, Belo Horizonte, MG, Brasil.

- Cunningham, M (2019). *Finite Element Model Validation and Testing of an Off-Road Vehicle under Dynamic Loading Conditions*. Doctoral Dissertations and Master's Theses. Embry-Riddle Aeronautical University, Daytona Beach, Flórida, EUA.
- English, & Hoffmann, K. (n.d.). *HBM Publication Practical Hints for the Installation of Strain Gages*. Retrieved April 11, 2023, from <https://www.hbm.com/fileadmin/mediapool/hbmdoc/technical/s1421.pdf>
- Gillespie, T. D. (2021). *Fundamentals of vehicle dynamics*. Society of Automotive Engineers.
- Hoffmann, K. (n.d.). https://www.hbm.com/fileadmin/mediapool/files/books/hoffmann-book/HBM_Karl-Hoffmann_An-Introduction-to-Stress-Analysis-using-Strain-Gauges.pdf
- Lee, Y.-L., Barkey, M. E., & Kang, H.-T. (2011). *Metal Fatigue Analysis Handbook*. Elsevier.
- Ltda, T. E. e C. (n.d.). *Target Normas: ABNT NBR NM-ISO 7500-1 NBRNM-ISO7500-1 Materiais*. [Www.normas.com.br](http://www.normas.com.br). Retrieved April 10, 2023, from <https://www.normas.com.br/visualizar/abnt-nbr-nm/23332/nbrnm-iso7500-1-materiais-metalicos-calibracao-de-maquinas-de-ensaio-estatico-uniaxial-parte-1-maquinas-de-ensaio-de-tracao-compressao-calibracao-do-sistema-de-medicao-da-forca>
- Lynx Tecnologia. (n.d.). [Www.lynxtec.com.br](http://www.lynxtec.com.br). Retrieved September 30, 2023, from <https://www.lynxtec.com.br>
- Micro-Measurements – VPG. *STRAIN GAGE INSTALLATION ON A SHAFT FOR TORQUE MEASUREMENT*. Retrieved April 11, 2023, from: https://www.youtube.com/watch?v=y-dDurbXv_o&t=288s.
- Pereira, L. F. M. (2019). *Aplicação de extensometria a suspensão de protótipo de fórmula SAE com auxílio de análise por elementos finitos*. Trabalho de Conclusão de Curso (Graduação), Universidade de Brasília, Faculdade de Tecnologia, Departamento de Engenharia Mecânica, Brasília, DF, Brasil.
- Silva, P. M, C. et al. Dimensionamento de Molas de Duplo Estágio para Veículos Tipo Baja Sae (2020). *XX CONEMI - Congresso Internacional de Engenharia Mecânica e Industrial, Brasília D.F.* <https://doi.org/10.18540/jcecvl9iss8pp16665-01e>
- Norton, R. L (2011). *Machine design: an integrated approach*. Prentice Hall.